[35] Kinetic Analysis of Bimolecular Hepatitis *delta* Ribozyme

By SIRINART ANANVORANICH, KARINE FIOLA, JONATHAN OUELLET, PATRICK DESCHÊNES, and JEAN-PIERRE PERREAULT

Hepatitis *delta* ribozymes are derived from the self-cleaving motifs found in the genome of defective hepatitis *delta* virus (HDV). In the presence of hepatitis B virus, infectious HDV particles are assembled as a ribonucleoprotein complex that includes multiple copies of *delta* antigen, hepatitis B surface antigen, and the circular 1.7-kb RNA single-stranded HDV genome. The circular HDV genome is highly self-complementary with a secondary structure that can be depicted as a rod shape composed of two domains, referred to as the viroid-like and protein encoding domains (Fig. 1A). During viral replication multimeric strands of both the genomic and antigenomic polarities are generated. Self-cleaving motifs located in the viroid-like domain on both the genomic and antigenomic strands subsequently cleave these multimeric strands, releasing unit-length monomers of both polarities. The resulting monomers are then ligated to produce circular conformers.

Following molecular cloning of the HDV genome,[1] the minimum contiguous sequence and secondary structure of this catalytic RNA were thoroughly characterized using a series of nested deletion mutants and nuclease mapping assays.[2] Genomic and antigenomic self-cleaving motifs exhibit similar secondary structures and catalytic activities[3] (Fig. 1B). Several different secondary structures have been predicted[4,5]; however, the pseudoknot structure proposed by Perrotta and Been[3] is the most commonly used. According to this secondary structure, four stems, named P1, P2, P3, and P4, are formed (Fig. 1B). The stems are joined by single-stranded regions called junctions named J1/2, J1/4, and J4/2, respectively. Crystallographic data have shown *cis*-acting genomic *delta* ribozyme to possess an additional stem, referred to as the P1.1 stem, generated by base pair interactions between the L3 loop and the J1/4 helix.[6] The cleavage of a phosphodiester bond located at the 5′-end of stem P1 gives rise to reaction products containing a 5′-hydroxyl and a 2′,3′-cyclic phosphate terminus. This reaction requires divalent

[1] S. Makino, M. F. Chang, C. K. Shieh, T. Kamahora, D. M. Vannier, V. Govindarajan, and M. M. C. Lai, *Nature* **329,** 343 (1987).
[2] H. N. Wu, Y. J. Lin, F. P. Lin, S. Makino, M. F. Chang, and M. M. C. Lai, *Proc. Natl. Acad. Sci. USA* **86,** 1831 (1989).
[3] A. T. Perrotta and M. D. Been, *Nature* **350,** 434 (1991).
[4] H. N. Wu, Y. J. Wang, C. F. Hung, H. J. Lee, and M. M. Lai, *J. Mol. Biol.* **223,** 233 (1992).
[5] A. D. Branch and H. D. Robertson, *Proc. Natl. Acad. Sci. USA* **88,** 10163 (1991).
[6] A. R. Ferre-D'Amare, K. Zhou, and J. A. Doudna, *Nature* **395,** 567 (1998).

0076-6879/01 $35.00

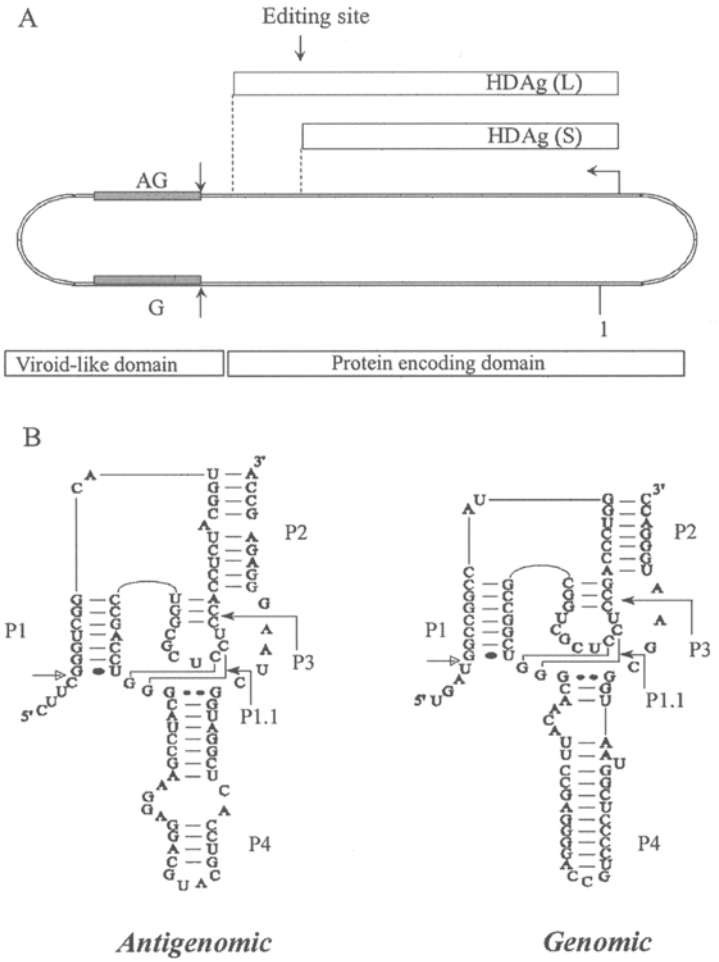

FIG. 1. (A) Schematic representation of the hepatitis *delta* virus (HDV) genome. Shaded boxes indicate the HDV self-cleaving motifs on genomic (G) and antigenomic (AG) strand. Clear boxes indicate the open reading frame of *delta* antigens (HDAg). The antigens are produced in two forms, either small (S) or large (L), as a consequence of an editing event occurring at the site indicated by an arrow. (B) Identification of the self-cleaving motifs on both the antigenomic and genomic single-stranded RNAs.

metal such as Mg^{2+}, Mn^{2+}, and Ca^{2+} and is referred to as *cis*-cleavage, in which the motif acts as a pseudoenzyme.

Based on the pseudoknot structure, a true enzyme, or *trans*-acting *delta* ribozyme, can be generated by eliminating a single-stranded junction so that one molecule acts as a substrate, while the other resulting molecule contains both the substrate binding site and catalytic domain (Fig. 2A). In our previous study we

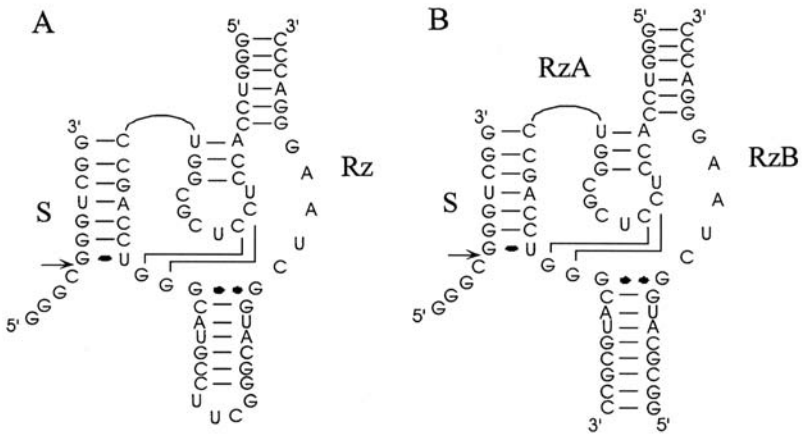

FIG. 2. (A) *Trans*-acting *delta* ribozyme derived from the antigenomic self-cleaving motif. (B) Bimolecular *delta* ribozyme system.

used a version derived from the antigenomic self-cleaving motif, with its J1/2 junction removed. In addition, stems P2 and P4 were shortened so that only minimum sequences remained, and the 5′-end sequence of the ribozyme began with GGG to ensure an efficient RNA production in *in vitro* transcription reactions. This *trans*-acting ribozyme derived from the *delta* ribozyme exhibits a unique characteristic in its substrate binding, namely that only the 3′-portion of the substrate is required for binding to the ribozyme. Specifically, a short stretch of nucleotides (7 nt) located on the substrate, which can be referred to as the ribozyme recognition site, is all that is required for binding. We view this characteristic as an advantage for the future development of a therapeutic means of controlling, for example, a viral infection. Moreover, when we thoroughly characterized the effect of neighboring sequences located on both ends of the recognition site, we found that the substrate specificity of *delta* ribozyme can be altered to accommodate the cleavage of a long mRNA molecule,[7] and can also be enhanced.[8,9]

This article was designed so that several techniques used in enzymatic studies on hepatitis *delta* ribozymes can be presented. In order not to repeat previous studies on *trans*-acting antigenomic *delta* ribozyme,[10,11] a bimolecular *delta* ribozyme is used in this study to illustrate techniques that include RNA production, ribozyme assembly, and both cleavage and kinetic studies. This bimolecular *delta*

[7] G. Roy, S. Ananvoranich, and J. P. Perreault, *Nucleic Acids Res.* **27,** 942 (1999).
[8] S. Ananvoranich, D. A. Lafontaine, and J. P. Perreault, *Nucleic Acids Res.* **27,** 1473 (1999).
[9] P. Deschênes, D. A. Lafontaine, S. Charland, and J. P. Perreault, *Antisense Nucleic Acid Drug Dev.* **10,** 53 (2000).
[10] S. Ananvoranich and J. P. Perreault, *J. Biol. Chem.* **273,** 13182 (1998).
[11] S. Mercure, D. A. Lafontaine, S. Ananvoranich, and J. P. Perreault, *Biochemistry* **37,** 16975 (1998).

ribozyme (Fig. 2B) is derived from the HDV antigenomic self-cleaving motif and can reconstitute its catalytic activity. Although an analogous system has previously been reported by Sakamoto *et al.*,[12] it was a mixture of both antigenomic and genomic sequences and was used for different purposes. Our findings on the bimolecular *delta* ribozyme derived from the antigenomic sequence are therefore worth presenting and comparing to the former system. Ultimately, we are striving to reach two goals: (i) to describe the methodology used; and (ii) to provide insight into some of the characteristics of the bimolecular *delta* ribozyme system.

Design of Bimolecular *delta* Ribozyme System

Based on the *trans*-acting version of *delta* ribozyme, a bimolecular version has been designed so that the ribozyme can be assembled using two molecules, referred to as RzA and RzB (Fig. 2B). RzA can act as a substrate binding moiety so that the antisense effect can be explored; RzB is required to reconstitute the enzymatic property of the ribozyme complex. This system might be worthwhile for further investigation of its therapeutic potential regarding to both antisense and ribozyme effects. In addition, because of their relatively small size, the transcripts can either be chemically synthesized at an affordable cost, or enzymatically produced using T7 RNA polymerase in an *in vitro* transcription reaction. For *in vitro* transcription reactions, individual pairs of deoxyoligonucleotides for RzA, RzB, or substrate are designed so that the sequence immediately downstream of the T7 RNA promoter is either CCC or CCG in order to produce the best yield as reported by Milligan *et al.*[13] As a result, the transcripts of RzA, RzB, and substrate contain either GGG or GGC at their 5′-ends.

Materials and Methods

Deoxyoligonucleotides

The oligonucleotides Oligo-T7 promoter, 5′-GTA ATA CGA CTC ACT ATA GGG-3′; Oligo-substrate, 5′-CCG ACC CGC CCT ATA GTG AGT CGT ATT AC-3′; Oligo-RzA,5′-GGC GCA TGC CCA GGT CGG ACC GCG AGG AGG TGG ACC CTA TAG TGA GTC GTA TTA C-3;′ Oligo-T7RzB, GTA ATA CGA CTC ACT ATA GGC-3′; Oligo-RzB, GGG TCC CTT AGC CAT GCG CCT ATA GTG AGT CGT ATT AC-3′ are synthesized, deprotected, and purified commercially (Gibco-BRL, Gaithersburg, MD). The oligonucleotide pair, Oligo-T7 promoter and Oligo-substrate, Oligo-T7 promoter and Oligo-RzA, and Oligo-T7RzB

[12] T. Sakamoto, Y. Tanaka, T. Kuwabara, M. H. Kim, Y. Kurihara, M. Katahira, and S. Uesugi, *J. Biochem.* **121,** 1123 (1997).

[13] J. F. Milligan, D. R. Groebe, G. W. Witherell, and O. C. Uhlenbeck, *Nucleic Acids Res.* **15,** 8783 (1987).

and Oligo-RzB are used to produce the 11-nt substrate, the 37-nt RzA and the 20-nt RzB, respectively.

Enzymatic RNA Synthesis

Substrate is prepared by denaturing the deoxyoligonucleotides (Oligo-substrate and Oligo-T7 promoter, 500 pmol) at 95° for 5 min in a 20 μl mixture containing 10 m*M* Tris-HCl pH 7.5, 10 m*M* $MgCl_2$, 50 m*M* KCl, and then slowly cooling to 37°. *In vitro* transcription reactions are carried out using the resulting partial duplex as the template in a solution containing 27 units RNAguard RNase inhibitor (Amersham Pharmacia, Piscataway, NJ), 4 m*M* of each rNTP (Amersham Pharmacia), 80 m*M* HEPES–KOH pH 7.5, 24 m*M* $MgCl_2$, 2 m*M* spermidine, 40 m*M* dithiothreitol (DTT), 0.01 unit pyrophosphatase (Roche Boehringer Mannheim), and 25 μg purified T7 RNA polymerase[14] in a final volume of 50 μl at 37° for 4 h. After incubation, the reaction mixtures are fractionated by denaturing 20% polyacrylamide gel electrophoresis (PAGE, 19 : 1 ratio of acrylamide to bisacrylamide) containing 45 m*M* Tris–borate pH 7.5, 7 *M* urea, and 1 m*M* EDTA. RzA and RzB are synthesized under conditions similar to those described above for substrate synthesis. Following electrophoresis, the reaction products are visualized by UV shadowing, the bands corresponding to the correct sizes of substrate, RzA or RzB cut out, and the transcripts eluted overnight at 4° in a solution containing 0.1% sodium dodecyl sulfate (SDS) and 0.5 *M* ammonium acetate, pH 7.0 (w/v). The eluted transcripts are precipitated by the addition of 0.1 volume of 3 *M* sodium acetate, pH 5.2 and 2.2 volumes of ethanol. Transcript yields are determined by UV spectroscopy at 260 nm.

Chemical RNA Synthesis

RzB transcripts containing individual deoxyribose residues in place of the ribose ones at positions 9 to 14, which span a single-stranded portion (J4/2) in the ribozyme complex, are chemically synthesized (Fig. 5, inset). The synthesis has been carried out by the Keck Oligonucleotide Synthesis Facility (Yale University, New Haven, CT) using β-cyanoethyl chemistry. The resulting RNA/DNA mixed oligonucleotides are deprotected as described by Perreault and Altman,[15] and purified on a PAGE gel.

End-Labeling of RNA with [γ-^{32}P]ATP

Purified transcripts (10 pmol) are dephosphorylated in a 20 μl reaction mixture containing 200 m*M* Tris-HCl pH 8.0, 10 units RNA Guard, and 0.2 units calf

[14] P. Davanloo, A. H. Rosenberg, J. J. Dunn, and F. W. Studier, *Proc. Natl. Acad. Sci. U.S.A.* **81,** 2035 (1984).

[15] J. P. Perreault and S. Altman, *J. Mol. Biol.* **226,** 399 (1992).

intestine alkaline phosphatase (Amersham Pharmacia). The mixture is incubated at 37° for 30 min, and then extracted twice with an equal volume of phenol : chloroform (1 : 1). Dephosphorylated transcripts (1 pmol) are 5′-end-labeled in a mixture containing 1.6 pmol [γ-^{32}P]ATP (6000 Ci/mmol), 10 m*M* Tris-HCl pH 7.5, 10 m*M* $MgCl_2$, 50 m*M* KCl, and 3 units T4 polynucleotide kinase (Amersham Pharmacia) at 37° for 30 min. Excess [γ-^{32}P]ATP is removed by spin chromatography through a Sephadex G-50 gel matrix (Amersham Pharmacia). The concentration of labeled transcripts is adjusted to 0.01 pmol/μl by the addition of water.

Nuclease Digestion and Alkaline Hydrolysis

The lengths and partial sequences of the RNAs are verified using specific cleavage by nucleases that digest ribose–phosphate backbones. Trace amounts of 5′-end-labeled RNA (<1 n*M*, *ca* 50,000 cpm) are dissolved in 4 μl of buffer containing 50 m*M* Tris-HCl, pH 7.5, 10 m*M* $MgCl_2$, and 100 m*M* NH_4Cl, and are then incubated at 37° in the presence of the ribonucleases. Ribonucleases T1 (Amersham Pharmacia), which digests Gp↓N in the single-stranded RNA, and U2 (Amersham Pharmacia), which preferably digests Ap↓N in the single-stranded RNA, are routinely used at final concentrations of 1 unit/μl. The reaction mixtures are incubated for 1 to 5 min at 37°. The cleavage reaction mixtures are fractionated on denaturing PAGE gels along with the corresponding RNA ladder. The ladders are generated by mixing, in a final volume of 5 μl, 5′-end-labeled RNA (50,000 cpm) in a solution containing 50 m*M* $NaHCO_3$ and 5 m*M* EDTA and incubating at 95° for 5 min. The reaction is quenched by the addition of 5 μl of loading buffer [95% formamide, 0.05% bromphenol blue, and 0.05% xylene cyanol (v/v)]. The reaction products and the ladders on the electrophoresed gels are visualized following the exposure of the gels to a phosphorimaging screen. The screens are then scanned and analyzed using ImageQuant version 5.0 (Molecular Dynamics, Sunnyvale, CA).

Determination of the Equilibrium Dissociation Constants (K_d)

In order to evaluate the assembly of the ribozyme complex, we have determined K_d values of both RzA : substrate and RzA : RzB complexes. The RzA : substrate equilibrium dissociation constant is determined by mixing individual RzA concentrations ranging from 0.1 to 300 n*M* with trace amounts of end-labeled substrate (<1 n*M*) in a 9 μl solution containing 50 m*M* Tris-HCl, pH 7.5. The mixtures are heated at 95° for 2 min, and then cooled to 37° for 5 min prior to the addition of $MgCl_2$ to 10 m*M* final, in a manner analogous to that of a regular cleavage reaction. The samples are incubated at 37° for 1.5 h, at which point 2 μl of sample loading solution [50% (v/v) glycerol, 0.025% of each bromphenol blue, and xylene cyanol] is added, and the resulting mixtures electrophoresed through a nondenaturing polyacrylamide gel [12% acrylamide with a 29 : 1 ratio of acrylamide to bisacrylamide, 45 m*M* Tris–borate buffer, pH 7.5, containing 10 m*M* $MgCl_2$ and 10% (v/v)

glycerol]. Polyacrylamide gels are prerun at 20 W for 1 h prior to sample loading, and are then electrophoresed at 15 W for 4.5 h at room temperature. Quantification of the amount of bound and free substrate is performed following the exposure of the gels to a phosphorimaging screen, and the screen is scanned and analysed using ImageQuant version 5.0 (Molecular Dynamics). The RzA : RzB complex K_d is determined by mixing either RzA or RzB concentrations that ranged from 0.1 to 300 n*M* with trace amounts of either end-labeled RzB or RzA, respectively, and following a procedure similar to that described above in order to determine $K_d{}^{\mathrm{RzA}}$ and $K_d{}^{\mathrm{RzB}}$, respectively.

Cleavage Reactions

Optimal ratios of substrate to RzA, and RzA to RzB, are determined by cleavage activity assessment following measurement of the equilibrium dissociation constants. Various concentrations of ribozymes are mixed with trace amounts of substrate (final concentration <1 n*M*) in an 18 μl reaction mixture containing 50 m*M* Tris-HCl, pH 7.5, and subjected to denaturation by heating at 95° for 2 min. The mixtures are quickly placed on ice for 2 min, and then equilibrated to 37° for 5 min prior to the initiation of the reaction. Unless stated otherwise, cleavage is initiated by the addition of $MgCl_2$ to 50 m*M* final concentration. The cleavage reactions are incubated at 37° and are followed for 3.5 h or until the end point of cleavage is reached. The reaction mixtures are periodically sampled (2–3 μ1), and these samples are quenched by the addition of 5 μl stop solution containing 95% formamide, 10 m*M* EDTA, 0.05% bromphenol blue, and 0.05% xylene cyanol. The resulting samples are analyzed on a 20% PAGE as described above. Both the substrate (11 nt) and the reaction product (4 nt) bands are detected using a Molecular Dynamic phosphorimager after exposure of the gels to a phosphorimaging screen.

Measurement of Cleavage Rate (k_{obs})

Unlabeled substrate is mixed with trace amounts of end-labeled substrate (<1 n*M*) to a final concentration of 50 n*M*, and then incubated with various ribozyme concentrations (50 to 500 n*M*). The fraction cleaved is determined, and the rate of cleavage (k_{obs}) obtained by fitting the data to the equation $A_t = A_\infty(1 - e^{-kt})$, where A_t is the percentage of cleavage at time t, A_∞ is the maximum percent cleavage (or the end point of cleavage), and k is the rate constant (k_{obs}). Each observed rate is calculated from at least two measurements. Values obtained from independent experiments vary less than 15%.

Mg^{2+} Requirement of Bimolecular Ribozyme System

The ribozyme system is studied by incubating the reaction mixtures with various concentrations of $MgCl_2$ (1 to 500 m*M*) in the presence of RzA and RzB

(1 : 3, 50 : 150 n*M*) with substrate (50 n*M*). The concentrations of Mg^{2+} at the half-maximal velocity are calculated.

Results and Discussion

RNA Production

Approximately 25 to 100 μg of RNA was recovered from a 50-μl *in vitro* transcription reaction and gel purification. When higher amounts of RNA were required, the reaction volume was proportionally increased. We observed that the sequence downstrem of the T7 RNA polymerase promoter has a drastic influence on the RNA yield.[13] The sequence of the RNA products were verified using RNase T1 and U2 digestions.

Ribozyme Assembly

Since the design of the bimolecular ribozyme system was based solely on the predicted secondary structure of the HDV self-cleaving motif, it is possible that the transcripts might adopt an alternative conformation in solution. In order to test for the presence of any alternative conformers, RzA, RzB, and a mixture of RzA and RzB were fractionated on a native gel. When the individual transcripts were tested, a single band was observed for each RNA species. The RzA–RzB complex was observed to migrate more slowly than the individual RzA and RzB transcripts. We also observed that approximately 2% of the end-labeled RzB behaved like another retarded complex migrating at the same level as the unbound RzA and lower than the RzA–RzB complex (Fig. 3A, indicated by an arrowhead). The amount of this unexpected band could not be accurately measured due to the elevated background level in the lanes.

Two independent experiments were performed using 11 different concentrations of either RzA or RzB against trace amounts of either RzB* or RzA* (the asterisk denotes 5′-end-labeled transcripts). The amount of expected complex formed was used to calculate the equilibrium dissociation constants that indicate the mutual affinity of the two components of the complex. The migration of end-labeled RzA is proportionally retarded in the presence of increasing amounts of RzB. The amounts of retarded complex (RzA : RzB) and unbound labeled RzA are determined and used to calculate the percentage of complex formed as a function of the RzB concentration. The data are then fit to the simple binding equation, RzA : RzB complex formed (%) = [RzB]/K_d + [RzB], in order to obtain the equilibrium dissociation constant (K_d^{RzB}), which indicates the concentration of RzB required to retard 50% of the end-labeled RzA. The values of K_d^{RzA} for RzB* and S* were determined in a similar fashion (Fig. 3B). The observed K_d values are similar (4 to 7 n*M*), suggesting that individual transcripts have similar affinities for the complex formation.

A

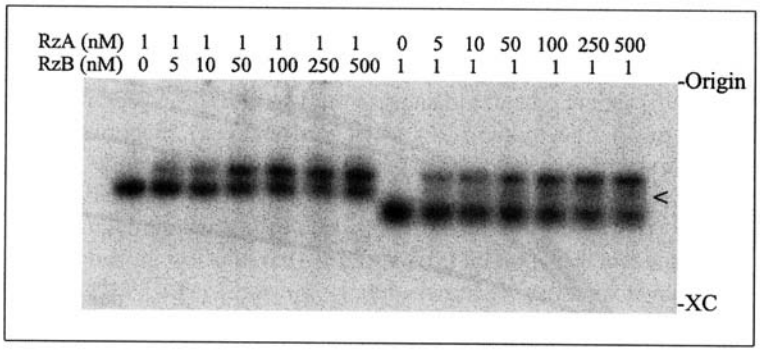

B

Equilibrium dissociation constants (K_d)	
K_d^{RzB} (RzA* and RzB)	6.7 ± 0.9 nM
K_d^{RzA} (RzB* and RzA)	4.4 ± 0.9 nM
K_d^{RzA} (S* and RzA)	6.6 ± 0.8 nM

FIG. 3. (A) Autoradiogram of a gel retardation assay used in the measurement of equilibrium dissociation contants. (B) Calculated values of K_d.

Ribozyme Cleavage

Native gel electrophoresis indicated that there is a low level of an alternative RzA–RzB complex formed in solution. Prior to performing the kinetic study, an optimal molar ratio of RzA and RzB was assayed using a cleavage assay. Time course experiments in which the amounts of substrate and RzA were kept equal (S : RzA, 1 : 1, 50 n*M*) and were incubated with increasing amounts of RzB (50 to 400 n*M*) were then performed. The fractions of product formed and substrate remaining were measured and plotted as a function of time as shown in Fig. 4A. Observed cleavage rates of $0.16 \pm 0.02 \text{min}^{-1}$ were observed for all mixtures, whereas maximal cleavage product levels were detected when the RzB concentration was higher than 150 n*M*, or when the ratio of S : RzA : RzB was 1 : 1 : 3. At lower RzB concentrations (50 to 100 n*M*), a suboptimal level of complex (S : RzA : RzB) was formed, resulting in the formation of lower amounts of product. In comparison to the

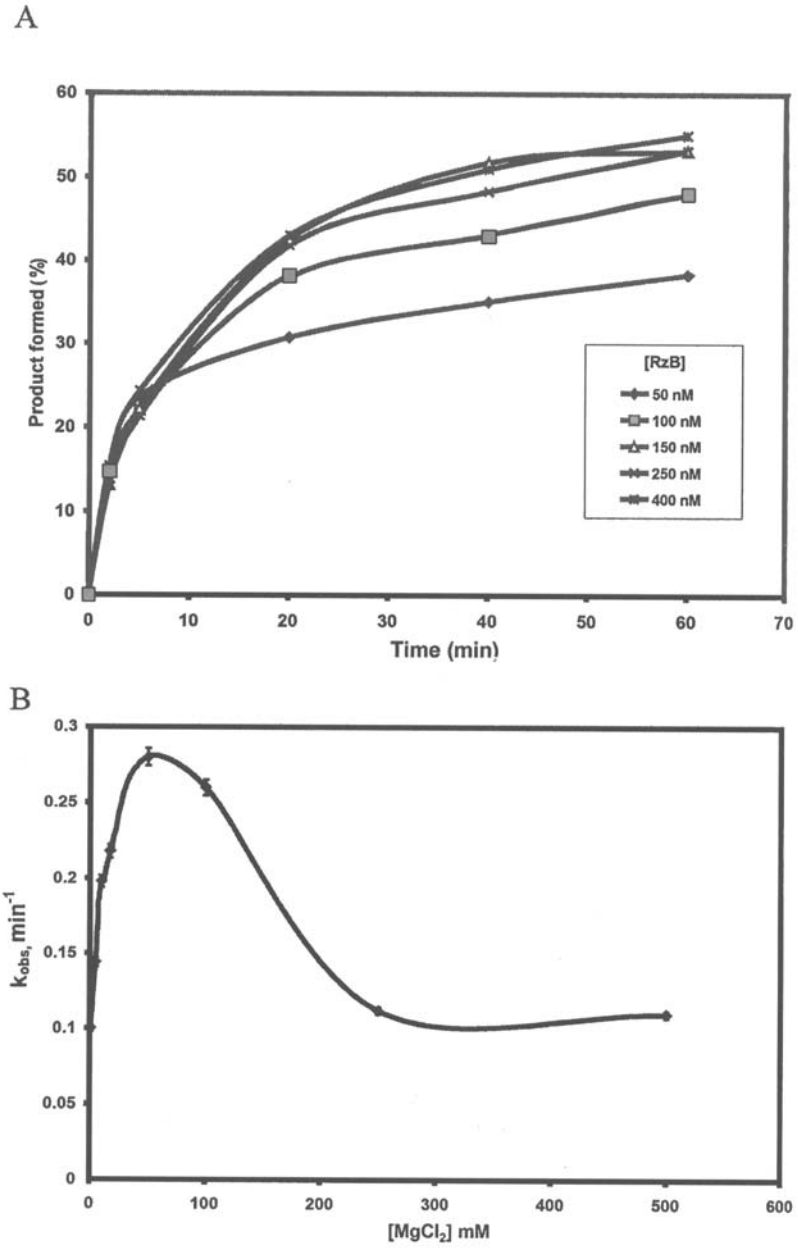

FIG. 4. (A) Time course experiments on the cleavage activity of assembled bimolecular systems containing 50 n*M* substrate and 50 n*M* RzA and various concentrations of RzB. (B) Determination of the $MgCl_2$ requirement of the bimolecular *delta* ribozyme in the presence of 50 n*M* of both substrate and RzA, and 150 n*M* RzB.

analogous system described by Sakamoto *et al.*,[12] higher ribozyme concentrations (RzA–RzB, 0.1 to 100 μM) were required in order to obtain a similar level of activity in the cleavage of substrate (0.1 μM). Since there was no detailed analysis on the previously reported ribozyme system, we assumed that alternative conformers are also present in the mixture and are responsible for the higher ribozyme concentration requirement. In comparison to the *trans*-acting *delta* ribozyme (whose structure is shown in Fig. 2A), the bimolecular ribozyme system has a similar observed rate of cleavage (i.e., 0.29 ± 0.2 min[1]) and 0.16 ± 0.2 min^{-1}, respectively. Although the maximum extent of cleavage of the bimolecular ribozyme is lower (60% of the substrate was cleaved), it has several features that encourage the further development of other ribozyme systems based on *delta* ribozyme structures (see below).

Magnesium Requirements of Bimolecular Ribozyme System

Similar to *cis*- and *trans*-acting *delta* ribozymes, the bimolecular ribozyme system requires divalent metal ions for its cleavage activity. More importantly, the bimolecular ribozyme might require higher concentration of metal ion for its assembly. For this reason we characterized its magnesium requirement. The optimal ratio of S : RzA : RzB (1 : 1 : 3) described earlier was used in cleavage reactions in the presence of various $MgCl_2$ concentrations (1 to 400 mM). When the values of k_{obs} were plotted as a function of magnesium concentration (Fig. 4B), the maximum cleavage rate was observed at 50 mM $MgCl_2$. These results are different from those of Sakamoto's system.[12] This might be due to the differences in the ratios of RzA, RzB, and total ribozyme used in the two studies.We suspect that the bell-shaped curve is due to the fact that higher $MgCl_2$ concentrations might promote the formation of an alternative conformation that yields no cleavage product. In order to determine the $MgCl_2$ concentration at which this occurs, other structural analyses are required.

Perspectives

The bimolecular *delta* ribozyme system possesses several interesting features that warrant further studies, including ones directed toward determining the structure–function relationship and developing an antisense/ribozyme dual system. For example, the construction of a miniribozyme with a higher stability (i.e., one resistant to nucleases) could be achieved using a similar strategy and introducing deoxyribonucleotides in place of the nuclease-sensitive riboses. With the generous contribution of a T7 RNA polymerase mutant by Dr. Rui Sousa (University of Texas Health Science Center, San Antonio, CA),[16] we have begun preliminary tests of a

[16] R. Padilla and R. Sousa, *Nucleic Acids Res.* **27,** 1561 (1999).

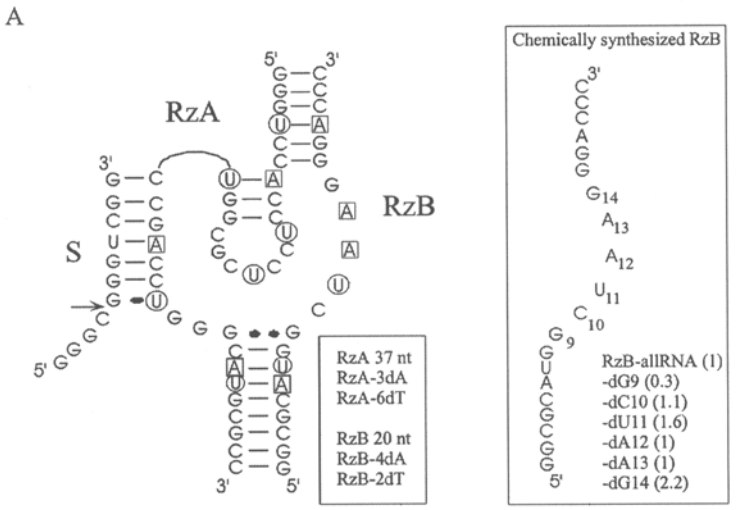

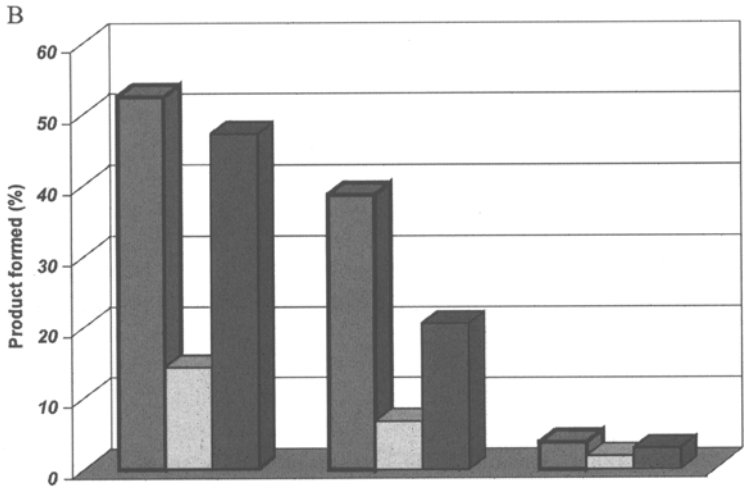

RzB \ RzA	all RNA	dA	dT
all RNA	52.5	38.7	3.8
dA	14.4	6.8	1.9
dT	47.3	20.6	3

FIG. 5. (A) Schematic representation of the RzA and RzB transcripts containing either single or multiple positions replaced with deoxyribose residues. Circled and boxed nucleotides represent the positions of replaced deoxyriboses. The extent of cleavage of singly substituted RzB transcripts are compared to chemically synthesized all RNA RzB (shown in the inset). The numbers in the brackets represent the relative extents of cleavage. (B) Histogram showing the extents of cleavage of RzA and RzB transcripts containing multiple substitutions.

mixed DNA/RNA bimolecular ribozyme system. This was achieved by substituting individual deoxyribonucleotides for ribonucleotides (at the same concentration) in *in vitro* transcription reactions using this mutant T7 RNA polymerase to produce RzA and RzB. The reactions using dATP and dTTP, to replace rATP and rUTP, respectively, produced RzA and RzB transcripts in comparable amounts as those using rATP and rUTP and wild-type T7 RNA polymerase. However, when either dGTP or dCTP was used, no RzA and RzB transcripts were produced. Most likely this is due to the greater number of guanidine and cytosine nucleotides in RzA and RzB. We then used the RzA and RzB transcripts containing dA and dT in a cleavage assay (Fig. 5). It should be noted that several positions on both RzA and RzB can be substituted by deoxyribose moieties. When the three adenine nucleotides of RzA are deoxyribose residues (RzA-3dA), RzB was observed to have a cleavage extent (38.7%) as compared to that of all RNA RzA and RzB (52.5%, Fig. 5B). The replacement of uracil by thymidine in the RzA transcript is detrimental to cleavage, most likely because the hydrogen bonds formed between these bases are impaired, specifically the wobble G-U base pair adjacent to the scissile phosphodiester bond. When the riboses of RzB were replaced by deoxyriboses (RzB-2dT), the ribozyme complexes of all RNA RzA and RzB-2dT result in 47.3% product formation, whereas RzB-4dA gave a lower cleavage extent (Fig. 5B).

In order to have a better understanding of the effect of the 2′-hydroxyl groups on the cleavage and assembly of the bimolecular ribozyme complex, single substitutions are required. According to the secondary structure, we suspect that the ribose residues of J4/2 might influence the formation of the RzA and RzB complex and its subsequent cleavage. Seven RzB transcripts possessing either all ribose residues or those with individual positions (9 to 14) replaced by deoxyribose residues were chemically synthesized (Fig. 5, inset). It should be noted that the chemically synthesized RzB exhibited slightly lower affinity for all RNA RzA, as well as a slightly lower activity than the enzymatically synthesized RzB. In order to have comparable values, all chemically synthesized transcripts including all RNA RzB were assayed with enzymatically synthesized RzA and substrate. When the extents of cleavage were compared, the presence of deoxyriboses at positions 10, 12, and 13 (RzB-dC10, -dA12, and -dA13) had no significant effect. RzB-dU11 and -dG14 promoted cleavage, whereas RzB-dG9 had a detrimental effect on it. Although we could not distinguish whether or not the 2′-hydroxyl group is important in the ability of RzB to form the complex, or in other interactions, we have initiated several studies on the structure–function relationship.

Conclusion

We described here the methodology used in the enzymatic study of a bimolecular ribozyme system derived from hepatitis *delta* ribozyme. The bimolecular ribozyme system is very promising for the further development of a mixed

RNA/DNA ribozyme system that is likely to be more stable to nuclease degradation than the all-RNA one.

Acknowledgment

This work was supported by a grant from the Medical Research Council (MRC) of Canada to J-P.P.